NASA TN D-787

C5
EXTRA COPY
C5

TECHNICAL NOTE

D-787

PILOTED SIMULATOR TESTS OF A GUIDANCE SYSTEM WHICH CAN CONTINUOUSLY PREDICT LANDING POINT OF A LOW L/D VEHICLE DURING ATMOSPHERE RE-ENTRY

By Rodney C. Wingrove and Robert E. Coate

Ames Research Center
Moffett Field, Calif.

LIBRARY COPY
JAN 15 1970
MANNED SPACECRAFT CENTER
HOUSTON, TEXAS

NATIONAL AERONAUTICS AND SPACE ADMINISTRATION
WASHINGTON March 1961

590328
36p.

NATIONAL AERONAUTICS AND SPACE ADMINISTRATION

TECHNICAL NOTE D-787

PILOTED SIMULATOR TESTS OF A GUIDANCE SYSTEM WHICH CAN CONTINUOUSLY PREDICT LANDING POINT OF A LOW L/D VEHICLE DURING ATMOSPHERE RE-ENTRY

By Rodney C. Wingrove and Robert E. Coate

SUMMARY

The guidance system for maneuvering vehicles within a planetary atmosphere which was studied uses the concept of fast continuous prediction of the maximum maneuver capability from existing conditions rather than a stored-trajectory technique. In the method of display and control used, desired touchdown points are compared with the maximum range capability and heating or acceleration limits, so that a proper decision and choice of control inputs can be made by the pilot.

A piloted fixed simulator was used to demonstrate the feasibility of the concept and to study its application to control of lunar mission re-entries and recoveries from aborts. A repetitive solution time on the order of 6 seconds was adequate for re-entries from satellite speeds where conditions were not changing rapidly, but for re-entry at parabolic speeds from lunar missions a faster solution time was indicated. The regions of entry conditions leading to control-sensitivity problems corresponded to trajectories which skipped up to the edge of the atmosphere. The simulation was also used to define the ground areas that would be attainable during typical entries using this method of guidance control for a vehicle with moderate lifting capability (lift-drag ratio of 0.5).

INTRODUCTION

Various systems have been studied for guiding maneuverable vehicles through a planetary atmosphere to a desired touchdown point without exceeding arbitrary temperature and acceleration limits. The concept of using perturbations about a fixed or stored trajectory has been considered in many studies (refs. 1 through 5 for example). These studies have shown that successful touchdown control with good precision can be achieved if the actual initial conditions of the entry are sufficiently near the stored values and if enough perturbation variables are used. The fixed-trajectory method is inherently limited, however, to the conditions and situations stored in the system.

Guidance systems for advanced missions may have to cope with wide variations in abort and entry conditions for nonstandard atmospheres. These requirements have stimulated interest in the possibilities of more "universal" system concepts that do not depend on stored conditions but, rather, continuously compute or predict the future trajectory from the present actual conditions. In addition to greater generality a continuous-prediction system might possess advantages in deriving and displaying hazardous flight regimes and in computing the total maneuvering capability to enable the pilot to decide upon alternate flight paths or destinations more easily.

From experience with fire-control systems it is inferred that one of the major problems in a continuous-prediction system will be the form of the equations used as a basis for the prediction computer. A satisfactory compromise must be achieved between the conflicting requirements for a reasonable amount of computing equipment, accuracy, speed, and realistic input information. To gain insight into these questions, a research program has been conducted with three goals: (1) to develop a continuous trajectory prediction technique, (2) to develop a display and control system to use the information generated, and (3) to study by means of an analog simulation how a pilot might be used to close the control loop and to assess the system capabilities. Since some of the need for generality in such a guidance system is associated with emergency or near-emergency conditions, the approach has been kept as simple as appeared feasible.

This report will describe in detail the equations used for the prediction of re-entry trajectories. The limitations and errors associated with the equations will be discussed along with a method of using this prediction scheme for re-entry control. The description and results of a piloted simulation are included to investigate the use of this guidance system for re-entry control. The re-entries simulated were both return trajectories from a lunar mission and trajectories that may occur in recoveries from aborts. No attempt has been made to match this terminal guidance system to particular midcourse guidance systems. It is assumed that the vehicle has arrived at the edge of the atmosphere within safe limits of entrance angles and velocities for the given vehicle.

NOTATION

A	acceleration factor, g units
b	span, ft
C_D	drag coefficient, $\frac{D}{qS}$
C_L	lift coefficient, $\frac{L}{qS}$

C_m	pitching-moment coefficient, $\frac{\text{pitching moment}}{qSc}$
C_n	yawing-moment coefficient, $\frac{\text{yawing moment}}{qSb}$
C_Y	side-force coefficient, $\frac{Y}{qS}$
c	mean chord, ft
D	drag force, lb
g	gravitation acceleration unit, ft/sec^2
h	altitude, ft
K_p, K_q, K_r	gain constants for simulated rate damping
K_{δ_a}, K_{δ_e}, K_{δ_r}	gain constants for simulated reaction controls
K	drag ratio in equation (5), $\frac{C_D \text{ for desired trim condition}}{C_D \text{ for existing trim condition}}$
L	lift force, lb
I_x, I_y, I_z, I_{xz}	moments of inertia about the x, y, and z axes and product of inertia about x and z axes, slug-ft^2
m	mass of vehicle, slugs
p', q', r'	rolling, pitching, and yawing angular velocities of body axes, radians/sec
q	dynamic pressure, $\frac{1}{2}\rho V^2$, lb/ft^2
r	distance from planet center, ft
R_X	downrange value along local great circle route in space, miles
R_Y	crossrange value normal to local great circle in space, miles
S	surface area, ft^2
t	time, sec

u	circumferential velocity component normal to radius vector, ft/sec
u_c	circular orbital velocity, $\sqrt{gr}$, ft/sec
$\bar{u}$	ratio, u/u_c
V	total velocity, ft/sec
Y	side force, lb
Z	dimensionless function of $\bar{u}$ determined by equation (1) and appropriate boundary conditions, $\frac{\rho\bar{u}}{2}\left(\frac{C_D S}{m}\right)\sqrt{\frac{r}{\beta}}$
α	angle of attack, radians
β	atmospheric density decay parameter, ft^{-1}, or sideslip angle, radians
δ_a, δ_e, δ_r	roll, pitch, and yaw controller deflections
γ	flight path angle relative to local horizontal direction; positive for climbing flight
ρ	atmosphere density, slugs/cu ft
φ	roll angle
θ	pitch attitude angle
ψ	lateral deflection angle

A
4
7
8

Subscripts

d	respect to destination
i	initial condition
max	trim for maximum L/D
min	trim for zero L/D
o	condition at roll angle, 0°
u	circumferential component normal to radius vector

X	along great circle route
Y	normal to plane of great circle route
x,y,z	respect to x, y, and z vehicle wind axes

BASIC CONCEPT

A478

For clarity a brief description of the final system concept is presented prior to the general discussion of the prediction equations, the display and control system, and the simulation results.

Figure 1 is a block diagram of a guidance and control loop containing the concepts studied in this report. An inertial platform and navigation computer continuously measures and computes the present flight conditions and destination information to feed to the prediction computer. The prediction computer continuously computes the maximum maneuver capability with respect to the destination (or destinations) and feeds this information to an automatic control system and a pilot's display. Either the automatic control system or the pilot, through an override, controls the vehicle to acquire and keep the destination in the center of the maximum maneuver capability envelope.

The elements considered in this report are the prediction computer and display. The function of the prediction computer is illustrated by figure 2 for a typical re-entry. From the existing vehicle condition, trajectories are computed for three constant trim values that give maximum downrange, minimum downrange, and maximum crossrange which are used to define the limits of predicted maximum range capability. The important point is that the differential equations of motion for the trajectories are solved by a "fast" computation in the airborne computer so that repetitive solutions are made continuously for the changing flight conditions.

The desired destination is also shown on figure 2. This information is located with respect to a nondimensionalized maximum range boundary and presented to the pilot by a typical display shown in figure 3. Thus, the pilot, by noting the destination with respect to his maneuver capability, can make a choice of control inputs.

Limits may be imposed on the range capability of a particular vehicle in the form of acceleration or heating boundaries or in the form of conditions for which the vehicle would "skip" out of the atmosphere in an undesired manner. With repeated prediction of total trajectories by fast computation, one or more of these limits can be indicated on the display, as shown by a typical boundary in figure 3, or fed to the automatic control system.

PREDICTION THEORY CONSIDERATIONS

Choice of Equations

The equations used for the prediction of range in this navigational method should, of course, be fairly general, be reasonably simple and accurate, use feasible inputs, and be suitable for rapid solution by the airborne computer. A closed-form solution of the range equation would be ideal, but no universal equation is known. The Sänger range equation for equilibrium glide (ref. 6) and the work of Eggers and Allen (ref. 7) give good closed-form solutions for high L/D vehicles with small flight path angles. The work of Allen and Eggers (ref. 8) gives a closed-form solution for zero L/D vehicles with large entrance angles. None of these equations could be considered universal enough for general range prediction, especially for low L/D (≈ 0.5) vehicles.

With no closed-form solutions, either stored empirical range data or fast computation of the equations of motion must be considered. Reference 5 describes a method of using linear prediction about stored trajectories. The method of storing complete nonlinear empirical range data in an airborne computer is feasible, but in order to cover many possible flight conditions and retain the desired generality, computing and storing this data would be a large task for each mission. It appears, then, that the fast solution of the trajectory motion would be the more desirable method to study.

First of all, to make the fast computation as simple as possible it is important to have simple equations which describe trajectory motion, and thus equations which only use those variables (such as velocity, flight path angle, altitude, deceleration, m/C_DS, and L/D) that strongly influence the vehicle maneuvering capability. Chapman (refs. 9 and 10) has set up a simple mathematical model which defines the important variables influencing re-entry trajectories. A comparison is made below of the quantities needed to describe a trajectory for standard computations and those needed for the Chapman mathematical model.

	Airborne measurements	Vehicle parameters
Standard	V, γ, h	m/C_DS , L/D
Chapman	V, γ, A_u	L/D

The Chapman model combines the vehicle's mass to drag ratio (m/C_DS) and altitude into a decleration measurement which gives an effective "density altitude." This density altitude is related through the Chapman equations with an exponential altitude-density variation.

There are three factors which make the use of the Chapman equations attractive for this application. First, the computations are simplified by the use of acceleration (density-altitude) inputs. Second, the relation between density and geometric altitude will be unknown during an actual entry; therefore the use of the effective density-altitude variation may provide a better basis for calculation on the usual nonstandard days. Third, the equations do not use geometric altitude as an input. Reference 11 shows that large errors may be present in the measurement of geometric altitude during a re-entry if an inertial platform is used in the loop. The Chapman equation, which uses the acceleration measurement instead of the geometric altitude, will not be strongly affected by this inertial platform error.

A
4
7
3

The basic Chapman equation from reference 9 used for trajectory prediction is shown below:

$$\bar{u}\,\frac{d^2Z}{d\bar{u}^2} - \frac{dZ}{d\bar{u}} + \frac{Z}{\bar{u}} - \frac{1 - \bar{u}^2}{\bar{u}Z} + \sqrt{\beta r}\left(\frac{L}{D}\right) = 0 \tag{1}$$

This nonlinear differential equation is solved repetitively during flight within an atmosphere. The solution is a variation in Z as a function of $\bar{u}$. To determine the downrange for each solution the following integration is made:

$$R_X = \frac{1}{5280}\,\frac{r}{\sqrt{\beta r}}\int_0^{\bar{u}_i}\frac{1}{Z}\,d\bar{u}\ ,\ \text{miles} \qquad r \approx 4000 \text{ miles for earth} \tag{2}$$

To determine the crossrange for each solution the following approximation, as described in reference 12, is used:

$$\left.\begin{aligned} R_Y &= \frac{1}{5280}\,\frac{r}{\sqrt{\beta r}}\int_0^{\bar{u}_i}\frac{\sin\psi}{Z}\,d\bar{u}\ ,\ \text{miles} \\ \text{with}\qquad & \\ \frac{d\psi}{d\bar{u}} &= -\frac{1}{\bar{u}}\,\frac{Y}{D} \text{ and } \frac{Y}{D} = \left(\frac{L}{D}\right)_0 \sin\varphi \end{aligned}\right\} \tag{3}$$

where $\varphi = 45^\circ$ and ψ is limited to 90° for maximum crossrange.

The constants assumed in the equations (r, $\sqrt{\beta r}$, $\sqrt{gr}$) will be a function of the particular planetary atmosphere in which the vehicle is operating. These studies use only the parameters for the earth's atmosphere but the computation procedure is perfectly general in this respect.

The initial conditions for the repetitive solutions of the nonlinear differential equations are taken from the velocity, flight-path angle, and acceleration measurements during the flight as follows:

$$\bar{u}_i = \frac{V \cos \gamma}{\sqrt{gr}}, \qquad \sqrt{gr} \approx 25{,}800 \text{ fps for earth} \tag{4}$$

$$Z_i = \frac{K(-A_u)}{\sqrt{\beta r}\ \bar{u}_i}, \qquad \sqrt{\beta r} \approx 30 \text{ for earth} \tag{5}$$

$$\left(\frac{dZ}{d\bar{u}}\right)_i = \sqrt{\beta r} \sin \gamma + \frac{Z_i}{\bar{u}_i} \tag{6}$$

The equation is solved for a constant (L/D) or, if needed, an L/D variation with velocity (to approximate L/D variation with Mach number for this solution). The factor K is used to correct the acceleration input from the drag value being held at the existing trim condition to the drag value for the desired trim condition for a computation. The value K can be made a constant equal to 1 for those vehicle configurations for which the resultant drag change is small compared with lift changes. For vehicles for which the drag change is large with changes in lift K can be made a function of the L/D (or α) being held. This K can also be used to find the trajectories resulting from the use of parachutes or drag-modulation controls to control the longitudinal accelerations such as outlined in reference 13.

Limitations of the Prediction Equations

The limitations of equation (1) for the prediction of trajectory motion are described in reference 9. An important limit on this solution is that it holds only for trajectory motions where appreciable drag exists. The absolute altitude limit is defined in detail in reference 9; to a first approximation equation (1) is good only for altitudes to about 300,000 feet from earth. In addition, throughout this report the approximate form for shallow entries has been obtained by setting $\cos \gamma = 1$, $\sin \gamma = \gamma$ and by disregarding L/D $\tan \gamma$ and $\tan^2 \gamma$ compared with unity. This small angle approximation generally indicates a better trajectory prediction capability during the first part of the manned re-entry trajectory when the flight path angles are small, as compared with the terminal portion of the trajectory (below about 100,000 ft), when the flight path angles become large.

The range quantities are predicted from an inertial cylindrical coordinate system based upon the instantaneous great circle route in space. The crossrange computed from this coordinate system is for a "flat earth" approximation away from the great circle. As reference 12 shows, this prediction is very good up to 1,000 miles crossrange on earth. Because the range solution is given for a great circle in space, the effect of the planet's rotation, with respect to the great circle, must be considered. The appendix indicates the effect of the planet's rotation on the range prediction and considers forms that may be used with the range prediction outlined above.

Any limitations on the longitudinal trajectory prediction can be eliminated by use of the full trajectory equation of motion transformed into $\bar{u}$ as the independent variable. For each particular re-entry problem it may be desirable to investigate additional terms, from the full equation, that could be added to equation (1) to extend the limits of the solution for the particular problem.

Error Analysis

A
4
7
3

End-point guidance errors associated with the prediction outlined above could come from many sources. The largest end point errors will come from the inertial platform and associated computer which gives the vehicle position and velocity vector relative to the earth destination. These errors, of course, will be a function of guidance components, accuracy of initial fixes, and the length of integrating time from these fixes.

The inertial-platform error analysis of reference 11 has been used here to indicate representative maximum prediction errors that might be expected with the trajectory prediction method of this report. A representative satellite re-entry of the $L/D = 0.5$ body, as outlined in reference 11, is shown in figure 4(a). In figure 4(b) the error introduced by the Chapman model (with no inertial-platform errors) has been determined from a comparison of the predicted range values with the range values for the complete equation of motion used in reference 11 for a standard density variation. It can be seen that during the latter portion of the trajectory below 100,000 feet, where the end-point error would be determined, the range prediction is within about 3.5 miles.

The maximum assumed inertial platform input errors which, when added together, give the maximum end-point errors have been taken from reference 11 as follows:

Initial altitude error	500 ft
Initial range to go error	-0.4 mile
Initial rate of climb error	1 ft/sec
Initial velocity error	-1 ft/sec
Acceleration bias	10^{-4} g
Gyro drift rate	$-2(10)^{-7}$ radian/sec

The effect of these errors in the prediction of range by the Chapman equation is shown in figure 4(c). It can be seen that the end-point error could be as much as 8.2 miles below 100,000 feet. The largest portion of this is the error of 4.8 miles in the range-to-go as determined from the inertial-platform computer. As can be seen from figure 4(a), there is a portion during this re-entry where there is typical radio blackout and little chance of up-dating the navigation information. Any up-dating that is possible during the re-entry would cut down the integrating time and thus cut down the navigation errors. These errors were calculated for a

constant L/D value. In the actual case, the end-point error would also be influenced by C_L and C_D variations in the low Mach number region, and would be influenced by the type of end-point landing devices, such as parachutes.

In addition to the end-point errors computed above, there are uncertainties which will affect the prediction of range by any method. These uncertainties are primarily the variations in density altitude profile that will occur from day to day and errors in the assumed aerodynamic coefficients which are approximated from test data.

It is important to bring out the fact here that because of the uncertainties in the range prediction listed above the computing errors in an actual airborne computer may be small in comparison. As shown in figure 1, a high accuracy computer, of the digital type, will be needed to give position information. In contrast, the guidance prediction computer can tolerate lower accuracies because it is continuously being fed corrected information and, as stated above, is predicting boundaries based on estimations. In the guidance prediction computer either an analog computer or a sufficiently fast digital computer could be used to solve the prediction equations.

DISPLAY AND CONTROL CONSIDERATIONS

This section will outline a general method of displaying and using for control the range prediction information obtained by the method outlined in the previous section.

Display

Destination and maneuvering capabilities.- A selected display has been shown previously in figure 3. The destination is presented on the pilot's display in relation to the predicted range capabilities of the vehicle, rather than in coordinates related to longitude and latitude on the surface of the earth. Three range values on the ground plane are used to fix the coordinate of the destination. The values used are two downrange quantities ($R_{X_{max}}$, $R_{X_{min}}$) and one crossrange quantity ($R_{Y_{max}}$). The destination is presented as a pip on a display where the coordinates of the the destination have been normalized in the following manner.

$$\text{Downrange position of destination} = \frac{R_{X_d} - R_{X_{min}}}{R_{X_{max}} - R_{X_{min}}} \tag{7}$$

$$\text{Crossrange position of destination} = \frac{R_{Y_d}}{R_{Y_{max}}} \tag{8}$$

Thus the display appears to the pilot as though he were looking through a window in the vehicle as it approaches its destination. The fixed face of the display indicates the locus of end-points, with respect to the destination, at which the vehicle would land if the given combination of roll angle and trim angle of attack (L/D) were held constant for the rest of the flight. An important assumption made in mechanizing this display is that the locus of end-points retains the same relative shape during the trajectory. The shape will be different for each particular vehicle because of different lift and drag characteristics. The constant relative shape for each particular vehicle has been found to be a good approximation for re-entry speeds less than satellite velocity. For speeds near or above satellite velocity the relative shape can change during the re-entry. The effect of uncertainties in the relative shape, in addition to the other uncertainties, such as density variation, aerodynamic characteristics and computing errors, does not create a substantial problem in the closed-loop control of range. This is because the pilot, in noting the drift of the destination position on the display, can make corrective control inputs about the predicted control input values to correct for the apparent drift. When the destination is in the center of the maneuver capability, the pilot has ±50 percent of the control capability available to make corrections. The uncertainties are critical during a re-entry when the pilot is asked to make a choice of destinations. Then the shape of the capability envelope and the effect of other uncertainties are of major importance and the pilot's choice of destination will only be as good as the prediction.

A
4
7
8

Flight envelope limits.- Each type of vehicle will have particular limiting flight conditions imposed by factors, such as heating and acceleration, that must be avoided. The possibility of adding this information to the display was considered. The same trajectory equations of motion that gave the range values also give values of acceleration and heating. It can be shown that the expressions derived in reference 9 for the deceleration, heating rate, and total heat input can be expressed in the following manner.

$$\text{Deceleration} = \text{Constant} \times \sqrt{1 + (L/D)^2}\ \bar{u}Z \tag{9}$$

$$\text{Heating rate at stagnation point} = \text{Constant} \times \bar{u}^{5/2}\ Z^{1/2} \tag{10}$$

$$\left.\begin{array}{l}\text{Total heat input per unit area}\\ \quad\text{at stagnation point}\end{array}\right\} = \text{Constant} \times \int_0^{\bar{u}_i} \frac{u^{3/2}}{\sqrt{Z}}\, d\bar{u} \tag{11}$$

The last two equations depend on the flow conditions assumed, and for this report are based on laminar boundry-layer flow with air as the working fluid.

If any of these quantities exceed the given limits during the prediction of the maximum or minimum values of downrange capability, control inputs could conceivably be made which would subsequently result in the vehicle's exceeding the limits. There are two ways that this information can be generated and given on the display to aid the pilot in control. First an L/D boundary marking which is some empirical function of the amount of overlimit can be mechanized on the display. Second, when the limits are exceeded, the next solution of the trajectory equation could use a $\Delta L/D$ value from the orginial L/D. In this manner the system would "hunt" for the L/D that would just reach the limit, and this value of L/D could be shown on the display as a boundary marking.

A limit that may be necessary is determined by the L/D value which would make the vehicle skip out of the atmosphere particularly for speeds near or above satellite velocity. This limit is especially important for systems based only on the solution of equation (1) because this solution does not hold for skip beyond the influence of aerodynamic acceleration forces. If it is desired to use the skip maneuver out of the sensible atmosphere to extend the range capability, then a suitable set of equations must be added to the prediction computer.

Control

One obvious method the pilot can use to control the flight path is to trim to the one combination of angle of attack and roll angle that the display indicates can be held constant to reach the destination. However, since the indicated trim conditions will probably change during the trajectory because of uncertainties in the prediction, changes from the original trim condition will usually be necessary.

Another method of control, which gives the largest safety margin for the uncertainties in the prediction, is to overcontrol and get the destination into the center of the predicted capabilities. Overcontrolling is done by trimming to the angle of attack for maximum maneuver capability holding the indicated roll angle out past the destination from the center of the display. When the destination pip comes to the center, the vehicle is then trimmed to the center of the capability thus leaving the maximum amount of control available for uncertainties.

How this method of re-entry control will tie in with a final landing or touchdown will depend upon the particular vehicle. A vehicle with conventional landing capability could use this method until it reached a beacon or landing flight path corridor (as outlined in ref. 14). Those vehicles which depend upon a parachute could use the prediction method in this report if a value of K in equation (5) were used which corresponded to the added drag of the parachute and $L/D = 0$ in equation (1).

The control of the vehicle along the trajectory will be affected by the time it takes for the repetitive solution of the trajectory equations. The time of solution gives an effective delay to the closed-loop control of the vehicle. The maximum allowable time will be a function of how rapidly the flight conditions change during the trajectory. For instance, slower solution times could be used for an equilibrium glider than for a low-lift vehicle entering the atmosphere at large flight path angles. A real time simulation study was made to gain some insight into the ability of this method of repetitive solution of trajectory equations in combination with the display system to give re-entry guidance control.

A
4
7
8

SIMULATION OF GUIDANCE METHOD

An analog flight simulation was made to investigate the use of the guidance method outlined above with example re-entry problems. The re-entries chosen were those that would be encountered by a lifting vehicle during a lunar mission. This investigation covered both re-entries into the earth's atmosphere with near-parabolic return velocity and re-entries for conditions that may occur from aborts during the boost trajectory.

Description of Simulation

The flight simulator consisted of a fixed cockpit in combination with an electronic analog computer. The flight simulator layout and display are shown in figures 5 and 6. As shown in figure 6 the pilot was given the following display information:

Trajectory position display:

- Velocity
- Altitude
- Rate of climb
- Acceleration
- Range to go

Short-period control display:

- Three body position angles
- Three body axis rates

Guidance display:

- Maximum maneuver capability and destination with boundary markings
- Bank angle
- Trim condition for L/D and corresponding angle of attack

The pilot control was applied through a two-axis side controller in combination with toe pedals. A block diagram of the analog simulation is shown in figure 7. The analog computer: (1) accepted control voltages from the pilot controls and solved the resulting vehicle's six-degrees-of-freedom motions; (2) computed the repetitive prediction equations; (3) generated the display information.

The vehicle equations of motion describe six-degrees-of-freedom dynamics along a great circle route (with small cross displacements) over the curved earth with no rotating atmosphere. The complete set of motion equations is shown in table I. The 1956 ARDC standard atmosphere was used in the computation of vehicle six-degrees-of-freedom motions. The altitudes simulated were from 100,000 to 300,000 feet because it is in this range that the major portion of the atmosphere entry is completed, and also because it was desirable in the analog simulation to keep the range of density variation as small as possible for scaling accuracy. The simulated mass parameters (table I) were based on the Project Mercury capsule but the lift and drag was assumed to be that of a flat plate nearly perpendicular to the airflow, with a maximum L/D of 0.5. Proportional reaction controls were simulated about the three axes. Constant-gain damping augmentation was included about the three axes so that the short-period damping would be near critical at the highest dynamic pressures. This damping along with very little coupling in the aerodynamics made the vehicle very stable in the short-period mode so that the pilot function was mainly one of guidance control.

A
4
7
8

The analog computer was programmed to solve equation (1) repetitively for the prediction of range and limits. The initial conditions for each solution were taken from equations (4), (5), and (6) with the value K of equation (5) used as 1. Because the analog computer was not equipped with high-speed computer components, the solution of the prediction equation could not be considered fast. The integration rate was $\int_{\bar{u}=1.4}^{\bar{u}=0} = 7$ seconds, in addition to a 1 second re-set time. This meant that the solution from parabolic velocity would be about 8 seconds, solutions from satellite velocity would be 6 seconds, and solutions from one-half satellite velocity would be 3.5 seconds. It can be seen that the solution was faster as the vehicle neared the destination. One of the items of interest in the simulation was the effect of this solution time. The method of predicting the maneuver capability is shown by a sketch in figure 8. The prediction of the minimum value of downrange was solved with $L/D = 0$ in equation (1). If the value of deceleration exceeded a given limit of 10 g along the trajectory, then an empirical relationship taken from references 9 and 10 was used to indicate on the display the minimum L/D that could be held without exceeding the 10 g limit. The prediction of the maximum downrange value was made with $L/D = 0.5$. If the maximum downrange trajectory skipped out of the atmosphere and thus went outside the region where equation (1) held, then the next repetitive solution included a value of $-\Delta L/D$ proportional to the amount of overshoot. Thus the repetitive calculation was continually hunting in a closed form for the L/D that would just stay within the atmosphere. The upper limit on the skip was taken as $Z \approx 0.0025$ which is equivalent to a deceleration of about 0.075 g

at satellite velocity. A boundary indicating the L/D that, if held, would just keep the vehicle within the atmosphere, was also shown on the display for pilot reference.

The guidance display used in this simulation is shown in figure 6. The "footprint," or range enveloped, was a transparent overlay on the face of a 5-inch oscilloscope. The destination pip and two boundaries were presented as moving quantities on the scope. Control information for the pilot was the bank indicator shown on the left and the trim position indicator shown on the right. This trim indicator shows the position of the trim control which regulates the trim angle of attack of the vehicle corresponding to an estimated trim L/D. The trim indicator as shown is scaled in both the angle of attack and L/D values. The bank indicator and trim indicator are correlated by the pilot to correspond to a trim position on the overlay. The pilot used the relationship of this trim position on the overlay with respect to the destination pip to control the vehicle.

A
4
7
8

Simulation Results

The problem of returning a vehicle from the moon through the earth's atmosphere has been studied in references 10, 15, and 16. Those studies have shown that the midcourse guidance system during the re-entry will have to keep the vehicle within a limit of safe atmosphere entrance angles. The re-entry trajectories for the simulation reported herein were initiated at 290,000 feet within the safe range of entrance angles. For those simulator runs initiated near the overshoot entrance angle, the skip boundary first appeared below $L/D = 0$ on the guidance display, thus indicating to the pilot that the vehicle should be rolled on its back (for negative lift) to stay within the atmosphere. For those simulated runs initiated near the undershoot entrance angle, the deceleration boundry first appeared at the top of the display, thus indicating to the pilot that trim conditions near maximum lift would have to be held during the initial descent to keep from exceeding the deceleration limit.

Maneuver capability.- Figure 9 shows re-entry trajectories for those entrance angles near the overshoot and undershoot limits. These particular trajectories were flown with the pilot holding the extreme trim conditions as indicated by the moving boundaries on the guidance display during a complete trajectory. The maximum range trajectory was flown with a skip to the edge of the atmosphere followed by trim at maximum L/D. The minimum range trajectory was flown by diving to the 10 g deceleration limit followed by trim at zero L/D. This minimum range could be made somewhat less by trimming at a value less than zero L/D to obtain a deceleration greater than that for trim at zero L/D. Figure 9(b) shows the ground area attainable by using the maximum capability of the vehicle, as determined by the guidance system. For any entrance within the given entrance angles the guidance system can direct the vehicle to any

destination within the overlap of the boundaries. A design end point to give the largest range margin to the guidance system would be in the center of the overlap of the boundaries.

Control problem areas.- Flying the trajectories along the lower acceleration boundary on the display gave no difficult control problems. The procedure was to hold trim conditions just above the acceleration boundary until the first dive into the atmosphere was checked and trim conditions near minimum range at $L/D = 0$ could safely be held. Flying to those destinations near the upper boundary, or for any trajectories where a skip up to the edge of the atmosphere (300,000 feet) was needed to extend the range, produced sensitive control problems. In particular, for these skipping trajectories, little control effectiveness was available near the top of the skip, so that the control obtained during the first dive into the atmosphere strongly influenced the rest of the trajectory. Figure 10 is presented to show those values of range and entrance conditions for which control was most sensitive, that is, where small errors in control resulted in large changes in range.

A
4
7
8

The sensitive control area includes those entrance angles from -2° to -3°. With these conditions the display indicated the vehicle would have to be rolled on its back (negative lift) to stay within the atmosphere. For these shallow entrance angles, small changes in control early in the trajectory with the vehicle on its back mean large changes in the skip trajectory. The indications of control inputs for these smaller entrance angles would be in the region below $L/D = 0$ on the display as shown in figure 6 so that no clear indication of proper control input was given to the pilot. It was the fault of the display then, as well as the sensitive control problem that made the shallow entry angles an unsatisfactory control region for precise control of range.

Figure 10, in addition to indicating the sensitive control areas, shows the usable range of entrance angles for this guidance system. The corridor limit on the left is a fuzzy boundary which is determined by the sensitive control problems for the shallow entrance angles. The corridor limit on the right is determined by the maximum deceleration value that can safely be tolerated by the vehicle and the crew. The maximum and minimum range boundaries shown in figure 10 were flown, respectively, for a skip to the edge of the atmosphere followed by trim at maximum L/D and for the dive to the maximum 10 g limit followed by trim at zero L/D. The region within these boundaries gives the control area that may be flown with this guidance system. The importance of extending the g-tolerance limit for the vehicle and crew can easily be seen in that it increases the usable area away from the control sensitivity problem region.

Pilot technique and opinion.- The method of pilot control in flying to an end point within the attainable ground area was as follows: During the first part of the trajectory when the vehicle was descending into the atmosphere, the pilot would trim at those conditions which the display indicated would get the vehicle to the destination. If the destination

signal appeared below the acceleration boundary, the pilot would trim just at the boundary. After the initial dive and the point of maximum deceleration was passed the pilot would overcontrol slightly to get the destination into the center of the range capability. Once the destination was in the center of the range capability, the pilot would trim to the indicated conditions and make small corrections for any drift away from the center during the rest of the trajectory. The pilots considered this guidance system satisfactory. In fact, the only pilot function needed was the simple one of closing the control loop between the bank and trim indicators and the navigation display. This meant changing trim conditions occasionally during the trajectory. Sophisticated problems requiring decisions or the selection of an alternate trajectory were not introduced in this early study.

The delay time due to repetitive solutions of the guidance equations did not particularly affect the control for those parts of the trajectory below satellite velocities during which flight conditions did not change rapidly. For those portions of the trajectory at parabolic re-entry velocities where the delay time was up to 8 seconds and where the conditions were rapidly changing during the initial descent, the delay time was considered unsatisfactory. Such a delay time would affect pilot control, though, only when the trim value held was appreciably different than that indicated to reach the destination. This meant the pilot had to trim to the value indicated to reach the destination rather than overcontrol when conditions were changing rapidly along the trajectory.

Effects of density variations.- The effect of unknown density variations on the guidance system is shown in figure 11. From the given entrance conditions, the pilot controlled to a given destination for a standard density variation and for density variations above and below the standard values. The nonstandard density values were introduced into the six-degrees-of-freedom equations as ±50 percent of the standard ARDC density at 300,000 feet with a linear percentage variation in the density to zero variation at 100,000 feet. As can be seen, the effect of density was mainly one of changing the geometric altitude trajectory profile. These density variations did not affect the display information and, in particular, did not appreciably affect the ability of the guidance system to compute the proper boundaries. This is due mainly to the fact, as pointed out earlier in the report, that this system uses the effective density altitude, instead of geometric altitude, for inputs to the computations.

Aborts from a boost trajectory.- Typical re-entries that would occur from a boost trajectory were also simulated. They not only show how this guidance system can be utilized during the boost portion of the mission, but also show how "universal" the system is for any entry into the earth's atmosphere. The typical boost trajectory chosen to be representative for the lunar mission is shown in figure 12. With this particular trajectory, if any aborts are made up to near the end of boost, the vehicle will enter

the atmosphere. Should there be an abort, it would be the job of this guidance system to furnish the information both for a choice of a particular landing point during the atmosphere portion of the entry and for control to that end point, without exceeding the acceleration limit. Two abort conditions from the boost trajectory were chosen for investigation. With the lower velocity, steep-descent entry the vehicle could conceivably exceed the acceleration limit of 10 g. With the higher speed abort, the vehicle could conceivably skip out of the atmosphere. Trajectories shown in figure 12(a) were controlled to the maximum maneuver boundaries as indicated on the guidance display. Figure 12(b) shows the ground area attainable for these entrance conditions. When the vehicle enters the atmosphere the pilot is able to choose a destination within this maximum capability and then control to that end point. The pilot control technique to a landing point during these aborts was similar to that for lunar mission re-entries, that is, trimming up to indicated values when the conditions were changing rapidly during the first of the trajectory, followed by overcontrolling during the rest of the trajectory to get and keep the destination in the center of the range capability.

Ames Research Center
National Aeronautics and Space Administration
Moffett Field, Calif., Jan. 18, 1961

APPENDIX

EFFECT OF PLANET ROTATION ON THE NAVIGATION SYSTEM

The planet's rotation, with respect to the vehicle's great circle route in space, will have two major effects on the navigation system. First the aerodynamic forces acting on the vehicle will be a function of the relative velocity between the inertial velocity of the vehicle and velocity of the air mass; and second, during the re-entry, the location of the destination will be changing, with respect to the vehicle's great circle route.

The relative velocity between the air mass and the vehicle can be approximated by letting the independent variable $\bar{u}$ of equation (1) be the sum, or difference, of the inertial velocity of the vehicle and the component of the planet's rotation, in the plane of the great circle at the destination. The $(1 - \bar{u}^2)$ term in equation (1) which contributes the inertial centrifugal force to the trajectory equation should contain the inertial velocity rather than the relative velocity. It is particularly important that the integral from zero to $\bar{u}_i$ in the prediction of range use the relative velocity so that $\Delta\bar{u} = 0$ when the vehicle reaches the destination.

To find the distance the destination will move during the re-entry relative to the great circle route in space it is necessary to know the time remaining during the trajectory. In reference 9 the following calculation of time for the solution of Z from equation (1) is derived

$$t = \frac{1}{\sqrt{\beta g}} \int_0^{\bar{u}_i} \frac{d\bar{u}}{\bar{u}Z} \text{ , sec}$$

The prediction for range in this report solves the Z function equation, not to the destination, but for constant trim conditions. A first-order approximation can be made that changes in time are proportional to changes in range and the following computation of time to destination is available.

$$t \approx \frac{\frac{1}{\sqrt{\beta g}} \int_0^{\bar{u}_i} \frac{d\bar{u}}{\bar{u}Z}}{\frac{r}{\sqrt{\beta r}} \int_0^{\bar{u}_i} \frac{d\bar{u}}{Z}} R_{X_d}(5280)$$

With this approximate form the corrected downrange position of the destination at the end of the trajectory is:

$$R_{X_d}' \approx R_{X_d} + \frac{u_{X_d} R_{X_d}}{\sqrt{gr}} \frac{\int_0^{\bar{u}_i} \frac{d\bar{u}}{\bar{u}Z}}{\int_0^{\bar{u}} \frac{d\bar{u}}{Z}}, \quad \text{miles}$$

where u_{X_d} is the velocity of the destination due to earth's rotation along the great circle route in space, fps.

The corrected crossrange prediction of the destination will be determined by the difference in the cross motion of destination due to planet rotation and the cross motion of the vehicle due to the cross movement of the air mass. During those portions of the trajectories in the atmosphere the two distances tend to cancel. For those trajectories that skip to the edge of the atmosphere the correction to the crossrange position of the destination becomes important. An approximate form of the corrected crossrange position can be determined from the derivation of time as outlined above combined with the derivation of crossrange from equation (8) with the corresponding approximation that crossrange is in proportion to downrange. For small lateral deflection angles ψ, and for the lateral force Y equal to $D(u_{Y_d}/u)$ then the corrected crossrange position of the destination is:

$$R_{Y_d}' = R_{Y_d} + u_{X_d} R_{X_d} \left[\left(\sqrt{gr} + \frac{1}{\sqrt{gr}} \right) \frac{\int_0^{\bar{u}_i} \frac{d\bar{u}}{\bar{u}Z}}{\int_0^{\bar{u}_i} \frac{d\bar{u}}{Z}} - \frac{\sqrt{gr}}{\bar{u}_i} \right], \quad \text{miles}$$

Correction of the touchdown point for the planet's rotation is an added refinement to the atmosphere re-entry portion of the navigation system and whether it is included or not would depend upon the type of re-entry trajectory. For instance, the length of time and the relative change in the position of the destination will be much smaller for those re-entries with large negative flight angles through the atmosphere, as opposed to those re-entries which glide along the edge of the atmosphere. Also, the orientation of the re-entry will determine whether the downrange or crossrange correction should be included. For instance, re-entry along a polar route would only need corrections to the crossrange, whereas re-entries along east-west routes would only need the downrange corrections.

REFERENCES

1. Eggleston, John M., and Young, John W.: Trajectory Control for Vehicles Entering the Earth's Atmosphere at Small Flight-Path Angles. NASA MEMO 1-19-59L, 1959.

2. Creer, Brent Y., Heinle, Donovan R., and Wingrove, Rodney C.: Study of Stability and Control Characteristics of Atmosphere-Entry Type Aircraft Through Use of Piloted Flight Simulators. IAS Paper No. 59-129, October 5, 1959.

A
4
7
8

3. Cheatham, Donald C., Young, John W., and Eggleston, John M.: The Variation and Control of Range Traveled in the Atmosphere by a High-Drag Variable-Lift Entry Vehicle. NASA TN D-230, 1960.

4. Assadourian, Arthur, and Cheatham, Donald C.: Longitudinal Range Control During the Atmospheric Phase of a Manned Satellite Reentry. NASA TN D-253, 1960.

5. White, J. A., Foudriat, E. C., and Young, J. W.: Guidance of a Space Vehicle to a Desired Point on the Earth's Surface. American Astronautical Society Preprint 61-41, 1961.

6. Sänger, Eugen: Raketen-flugtechnik. R. Oldenbourg (Berlin) 1933.

7. Eggers, Alfred J., Jr., Allen, H. Julian, and Neice, Stanford E.: A Comparative Analysis of the Performance of Long-Range Hypervelocity Vehicles. NACA TN 4046, 1957.

8. Allen, H. Julian, and Eggers, A. J., Jr.: A Study of the Motion and Aerodynamic Heating of Missiles Entering the Earth's Atmosphere at High Supersonic Speeds. NACA TN 4047, 1957.

9. Chapman, Dean R.: An Approximate Analytical Method for Studying Entry Into Planetary Atmospheres. NASA TR R-11, 1959. (Supersedes NACA TN 4276)

10. Chapman, Dean R.: An Analysis of the Corridor and Guidance Requirements for Supercircular Entry into Planetary Atmospheres. NASA TR R-55, 1959.

11. White, John S.: Investigation of the Errors of an Inertial Guidance System During Satellite Re-Entry. NASA TN D-322, 1960.

12. Slye, Robert E.: An Analytical Method for Studying the Lateral Motion of Atmosphere Entry Vehicles. NASA TN D-325, 1960.

13. Levy, Lionel L., Jr.: An Approximate Analytical Method for Studying Atmosphere Entry of Vehicles With Modulated Aerodynamic Forces. NASA TN D-319, 1960.

14. Bray, Richard, S., Drinkwater, Fred J., III, and White, Maurice D.: A Flight Study of a Power-Off Landing Technique Applicable to Re-entry Vehicles. NASA TN D-323, 1960.

15. Wong, Thomas J., and Slye, Robert E.: The Effect of Lift on Entry Corridor Depth and Guidance Requirements for the Return Lunar Flight. NASA TR R-80, 1960.

16. Hildebrand, Robert B.: Manned Re-entry at Super-Satellite Speeds. IAS Paper No. 60-83, 1960.

TABLE I.- SIMULATED MOTION EQUATIONS

Wind axis force equations:

$$\dot{V} = \frac{-qSC_D}{m} - g \sin \gamma$$

$$\dot{\beta} = \frac{qSC_Y}{Vm} + \frac{g}{V} \cos \gamma \sin \varphi + p' \sin \alpha - r' \cos \alpha$$

$$\dot{\alpha} = \frac{-qSC_L}{Vm} + \frac{g}{V} \cos \gamma \sin \varphi + q'$$

Body axis moment equations:

$$\dot{p}' = K_{\delta_a}\delta_a - K_p p'$$

$$\dot{q}' = \frac{qScC_m}{I_y} + \frac{I_z - I_x}{I_y} p'r' + K_{\delta_e}\delta_e - K_q q'$$

$$\dot{r}' = \frac{qSbC_n}{I_z} - \frac{I_y - I_x}{I_z} p'q' + K_{\delta_r}\delta_r - K_r r'$$

Wind axis Euler angles:

$$\dot{\varphi} = p' \cos \alpha + r' \sin \alpha + \dot{\psi} \sin \gamma$$

$$\dot{\gamma} = -\frac{1}{V}\left(A_z \cos \varphi + A_y \sin \varphi\right) + \frac{V \cos \gamma \cos \psi}{r + h}$$

$$\dot{\psi} = \frac{1}{V \cos \gamma}\left(A_y \cos \varphi - A_z \sin \varphi\right)$$

$$A_y = \frac{1}{m}\left(qSC_y + mg \cos \gamma \sin \varphi\right)$$

$$A_z = \frac{1}{m}\left(-qSC_L + mg \cos \gamma \cos \varphi\right)$$

Displacements:

$$R_{X_d} = \left[\left(R_{X_d}\right)_i - \int_0^t V \cos \gamma \cos \psi \, dt\right] \cos \psi$$

$$+ \left[\left(R_{Y_d}\right)_i - \int_0^t V \cos \gamma \sin \psi \, dt\right] \sin \psi$$

TABLE I.- SIMULATED MOTION EQUATIONS - Concluded

$$R_{Y_d} = \left[\left(R_{Y_d}\right)_i - \int_o^t V \cos \gamma \sin \psi \, dt\right] \cos \psi$$

$$- \left[\left(R_{X_d}\right)_i - \int_o^t V \cos \gamma \cos \psi \, dt\right] \sin \psi$$

$$h = h_i + \int_o^t V \sin \gamma \, dt$$

Vehicle aerodynamics:

$$\frac{C_L S}{m} = -0.673 \sin \alpha$$

$$\frac{C_D S}{m} = 0.673 \cos \alpha \qquad + 10 > \alpha > -26.5^\circ$$

$$\frac{C_m S c}{I_y} = -0.0678 \, \alpha$$

$$\frac{C_n S b}{I_z} = -0.0678 \, \beta$$

$$\frac{C_Y S}{m} = -0.673 \, \beta$$

$$I_{xz} = 0$$

$$\frac{I_z - I_x}{I_y} = \frac{I_y - I_x}{I_z} = 0.40$$

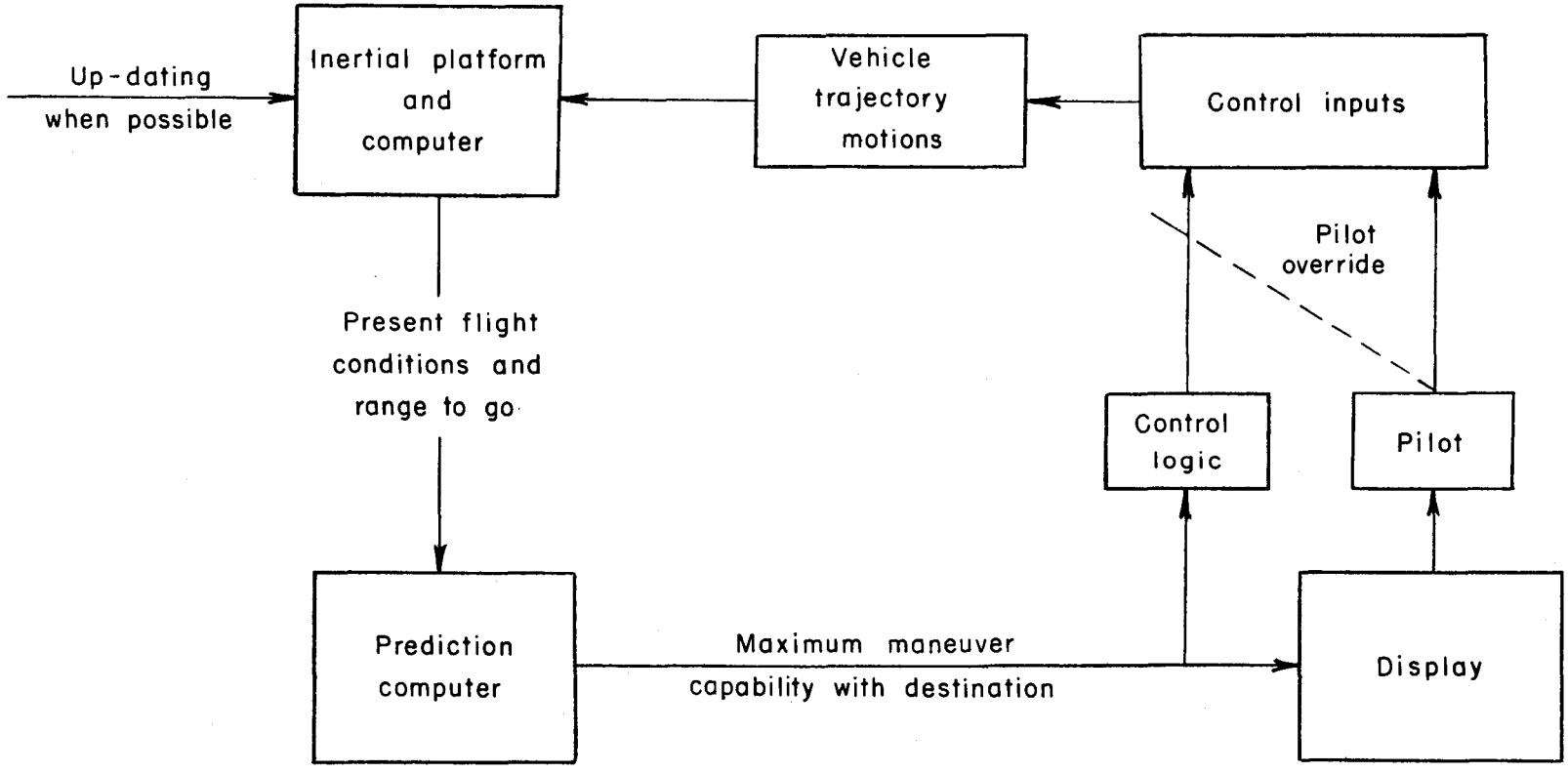

Figure 1.- Proposed navigation concept.

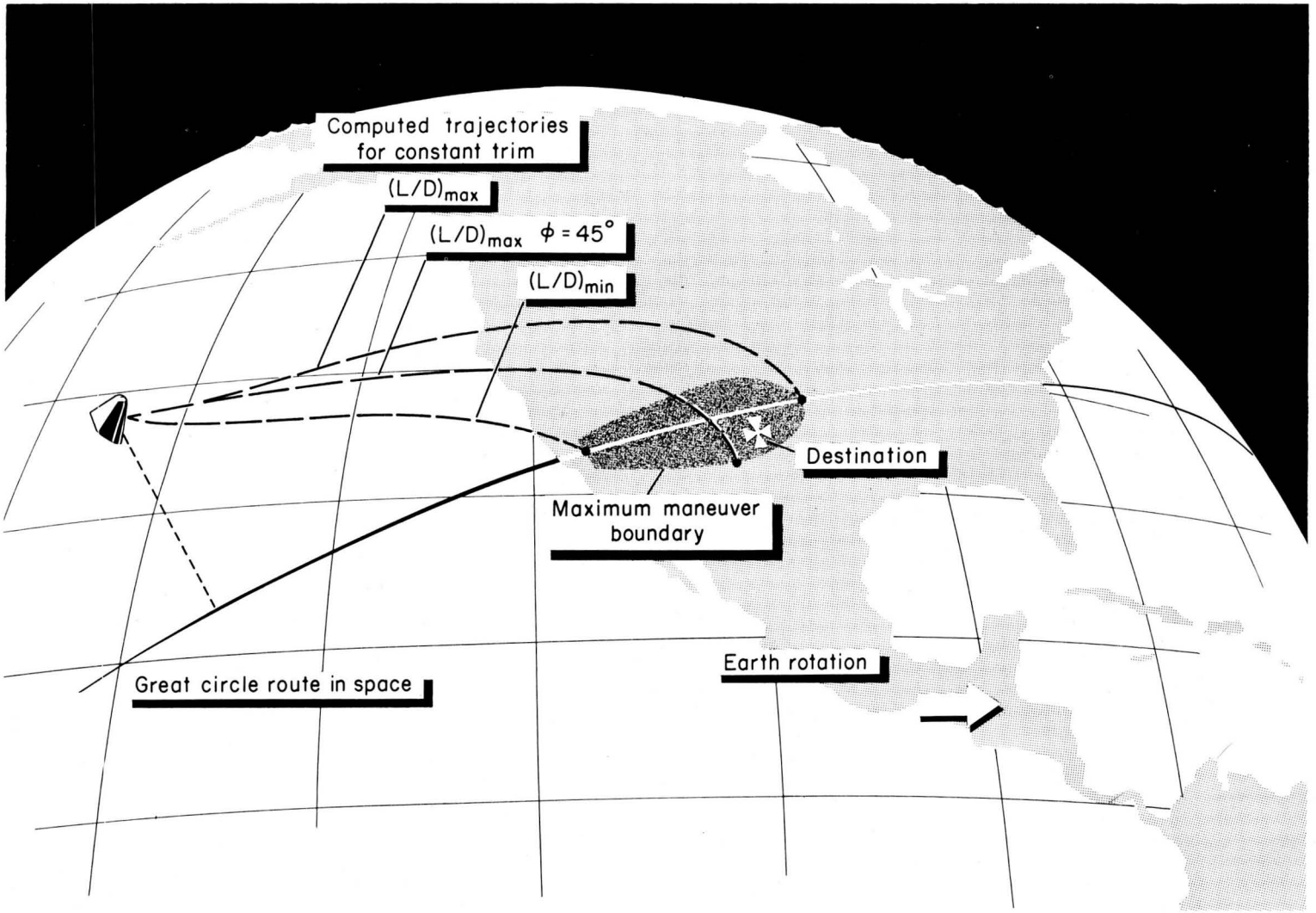

Figure 2.- Prediction method for the maximum maneuver capability.

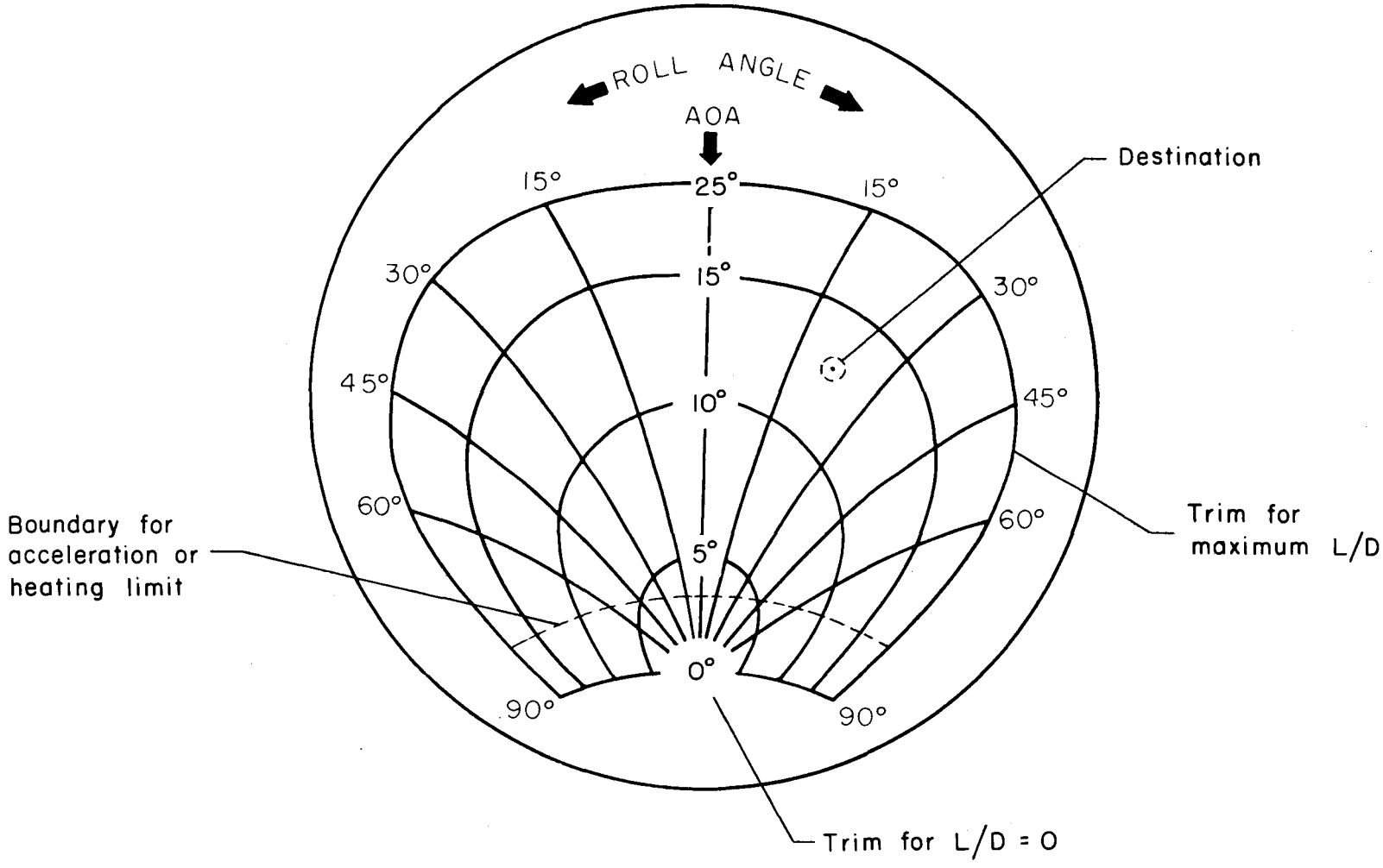

Figure 3.- Re-entry guidance display showing the destination with respect to the maneuver capabilities of the vehicle.

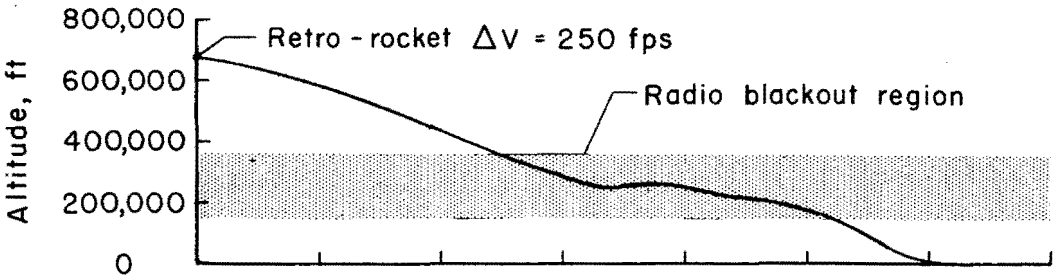

(a) Altitude time history.

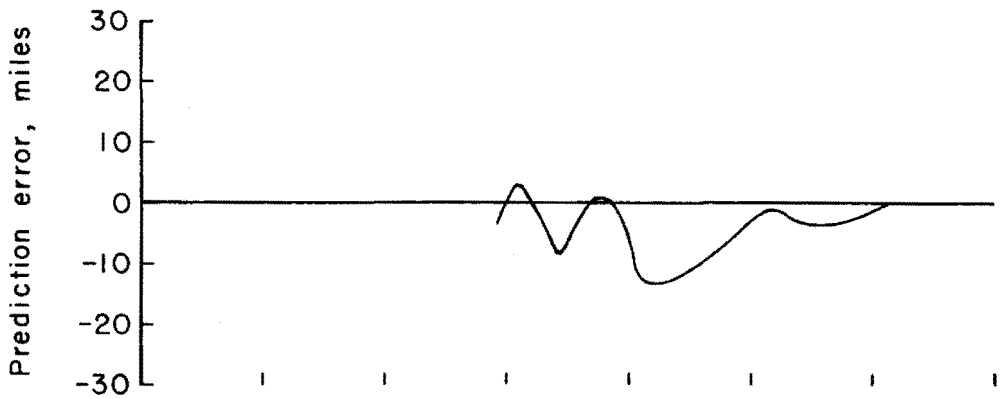

(b) Prediction error without inertial platform errors.

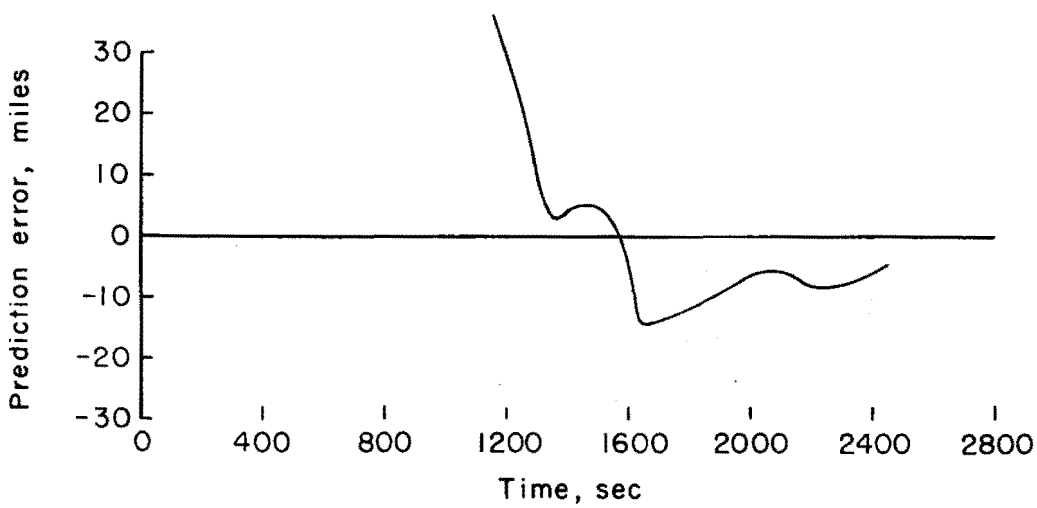

(c) Prediction error with inertial platform errors.

Figure 4.- Satellite re-entry trajectory with calculation of maximum prediction errors; $C_D S/m = 0.533$, $L/D = 0.5$.

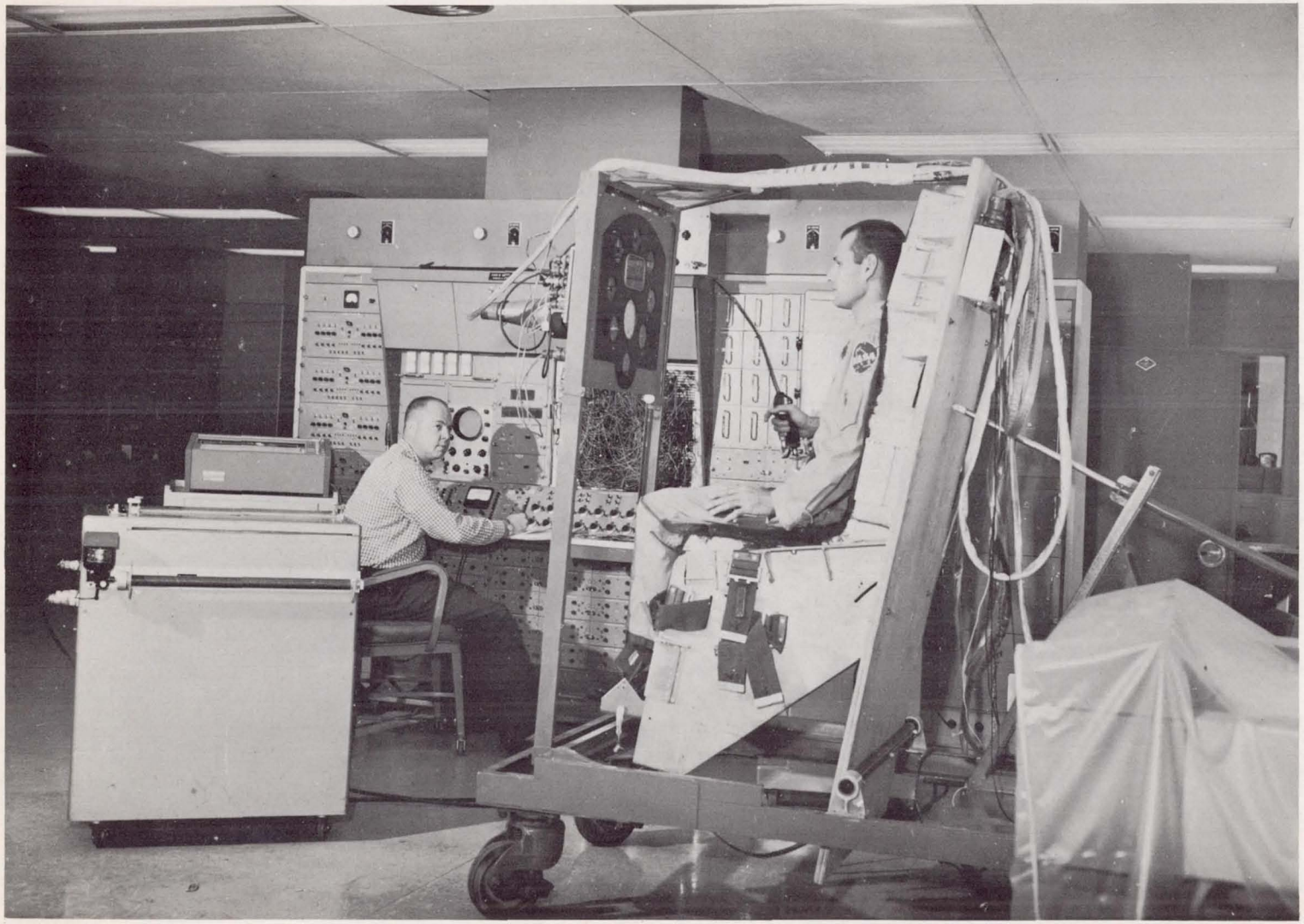

A-27105

Figure 5.- Over-all view of cockpit and analog computer.

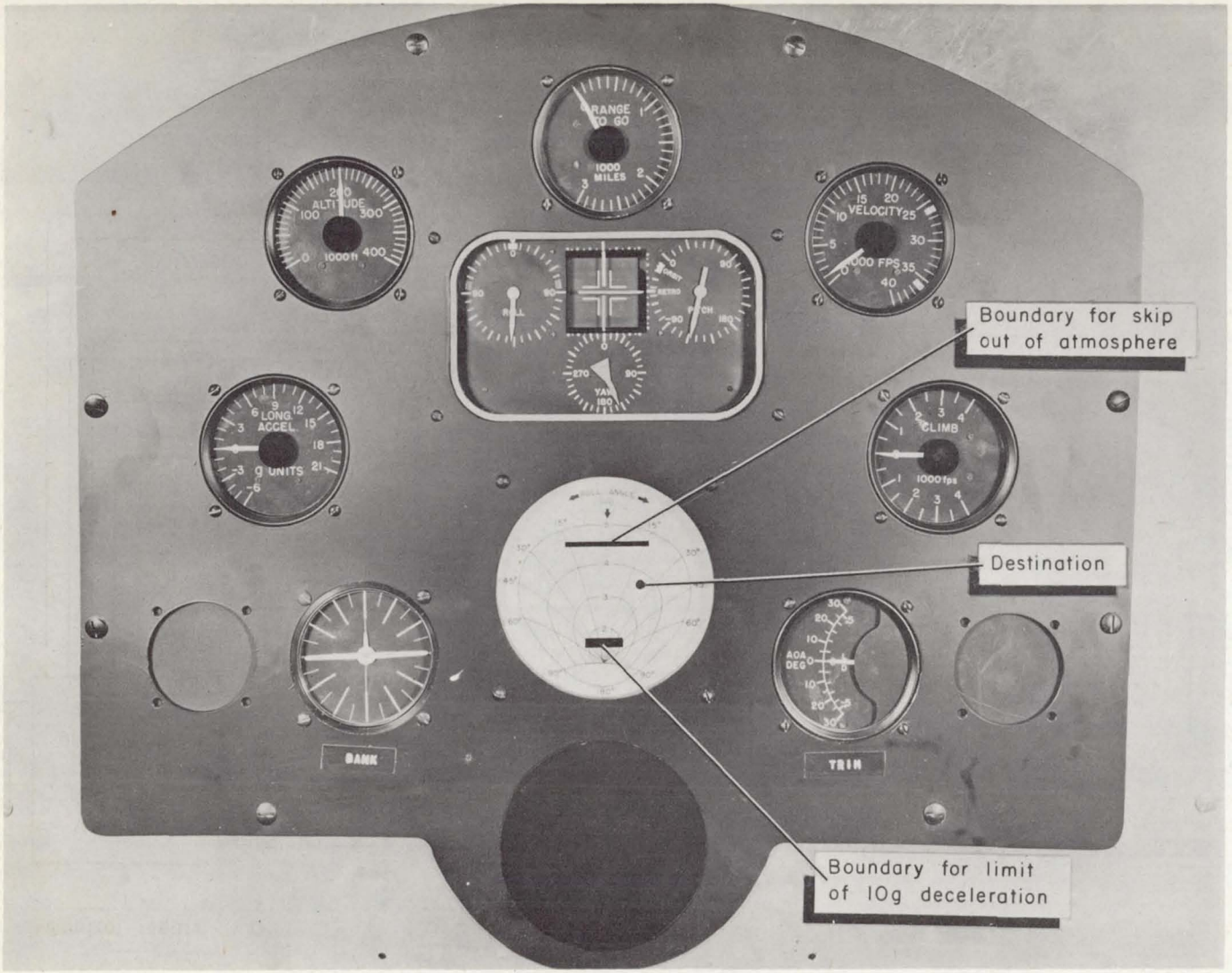

Figure 6.- Pilot instrument display.

A-26966.1

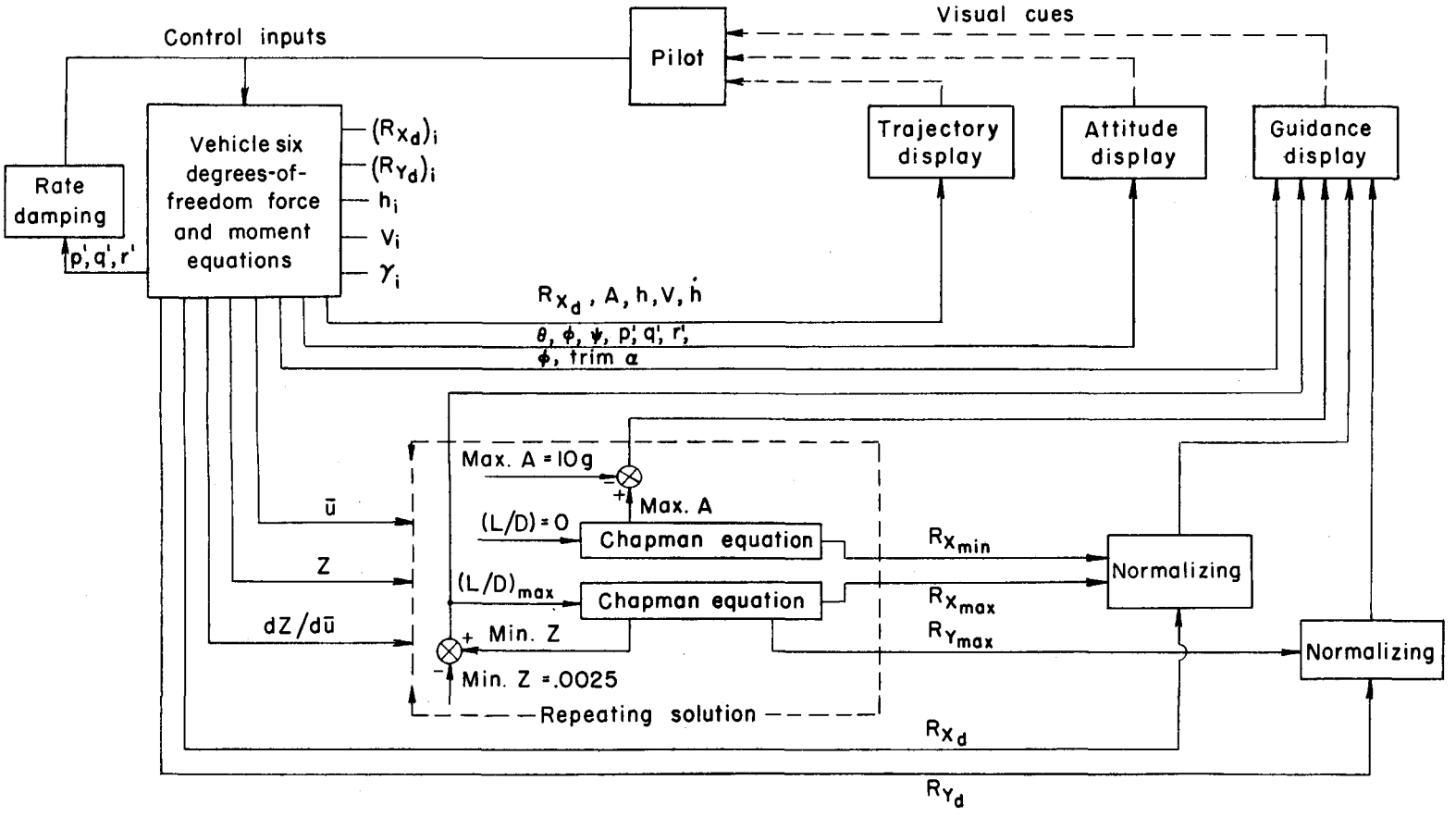

Figure 7.- Block diagram of the analog simulation.

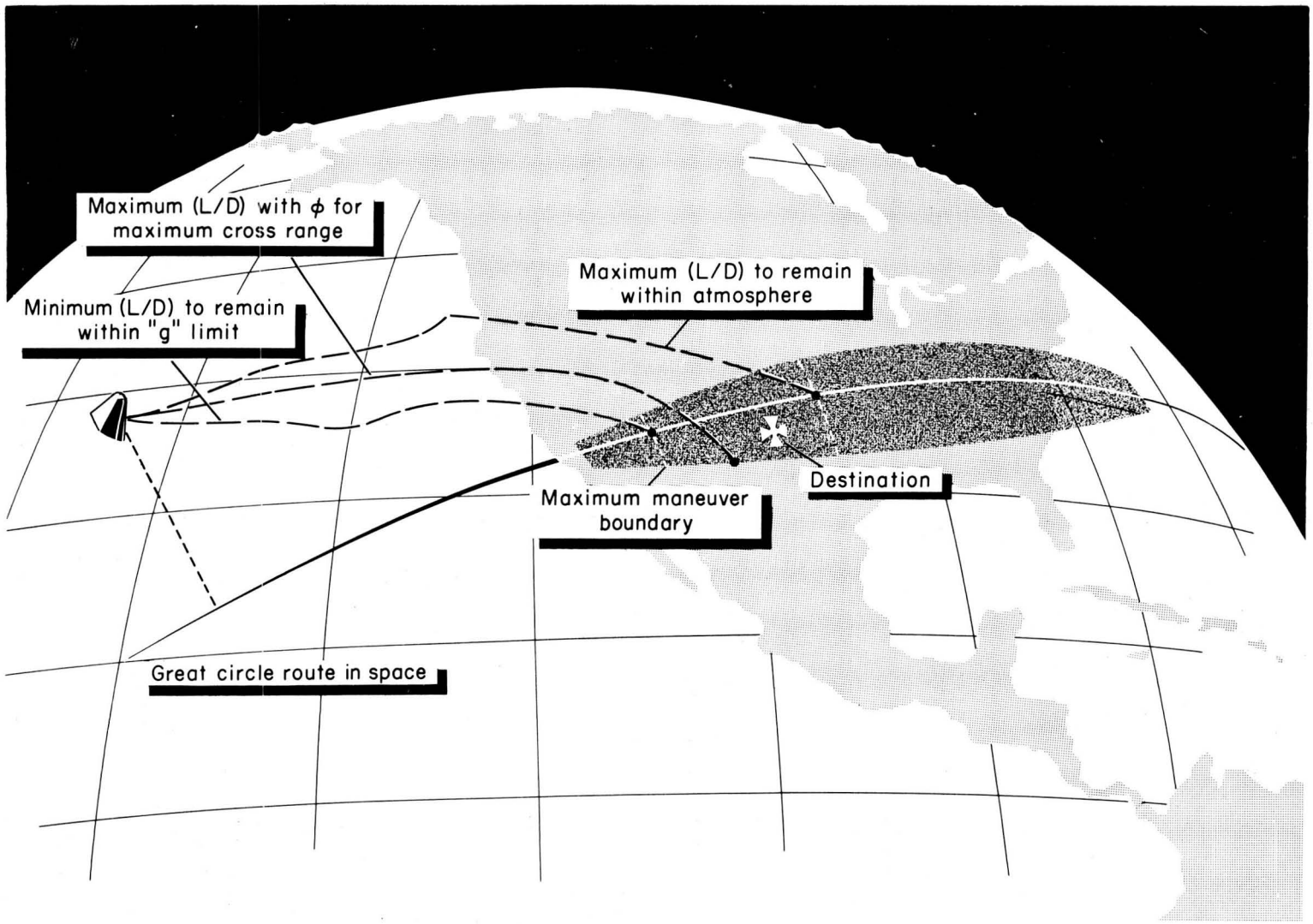

Figure 8.- Method of predicting the maximum maneuver capability for the lunar mission re-entries.

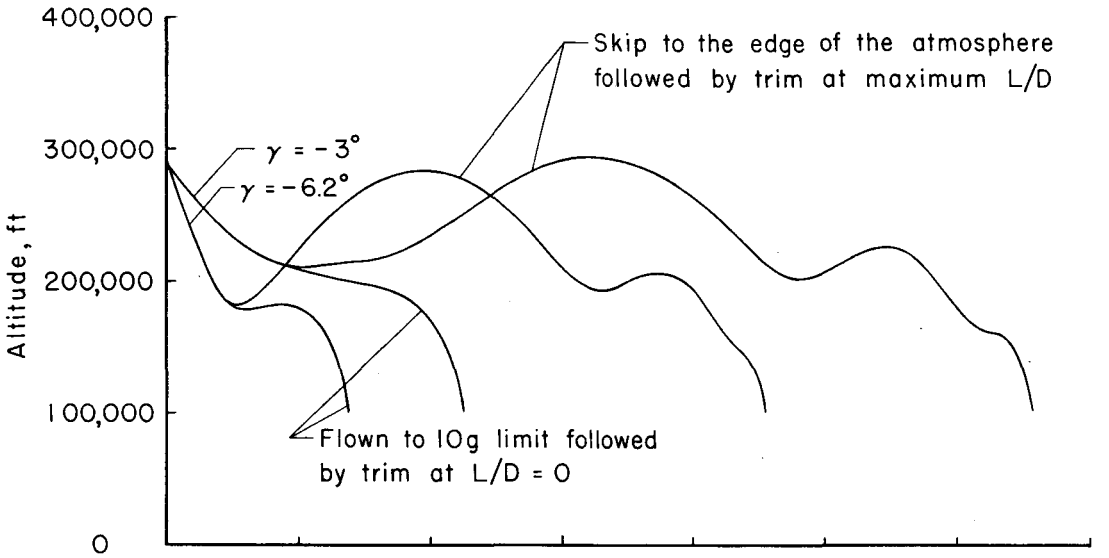

(a) Variation of range with altitude.

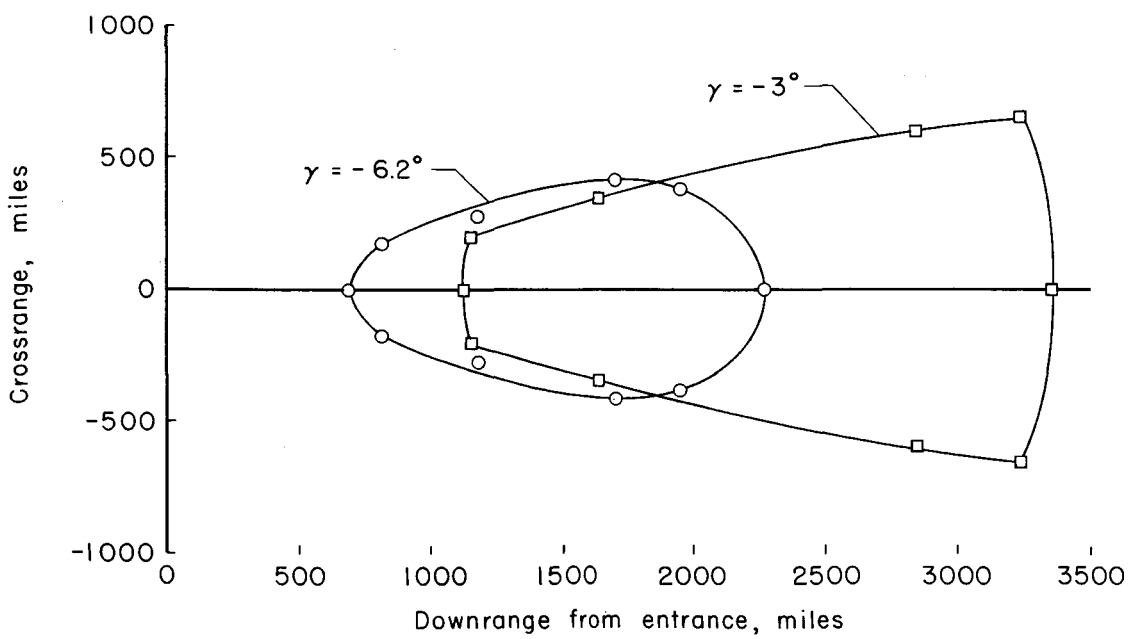

(b) Ground area attainable.

Figure 9.- Piloted trajectories from lunar mission re-entries. Entry conditions: V = 35,000 feet per second, h = 290,000 feet, $\gamma = -3^{\circ}$ and -6.2°.

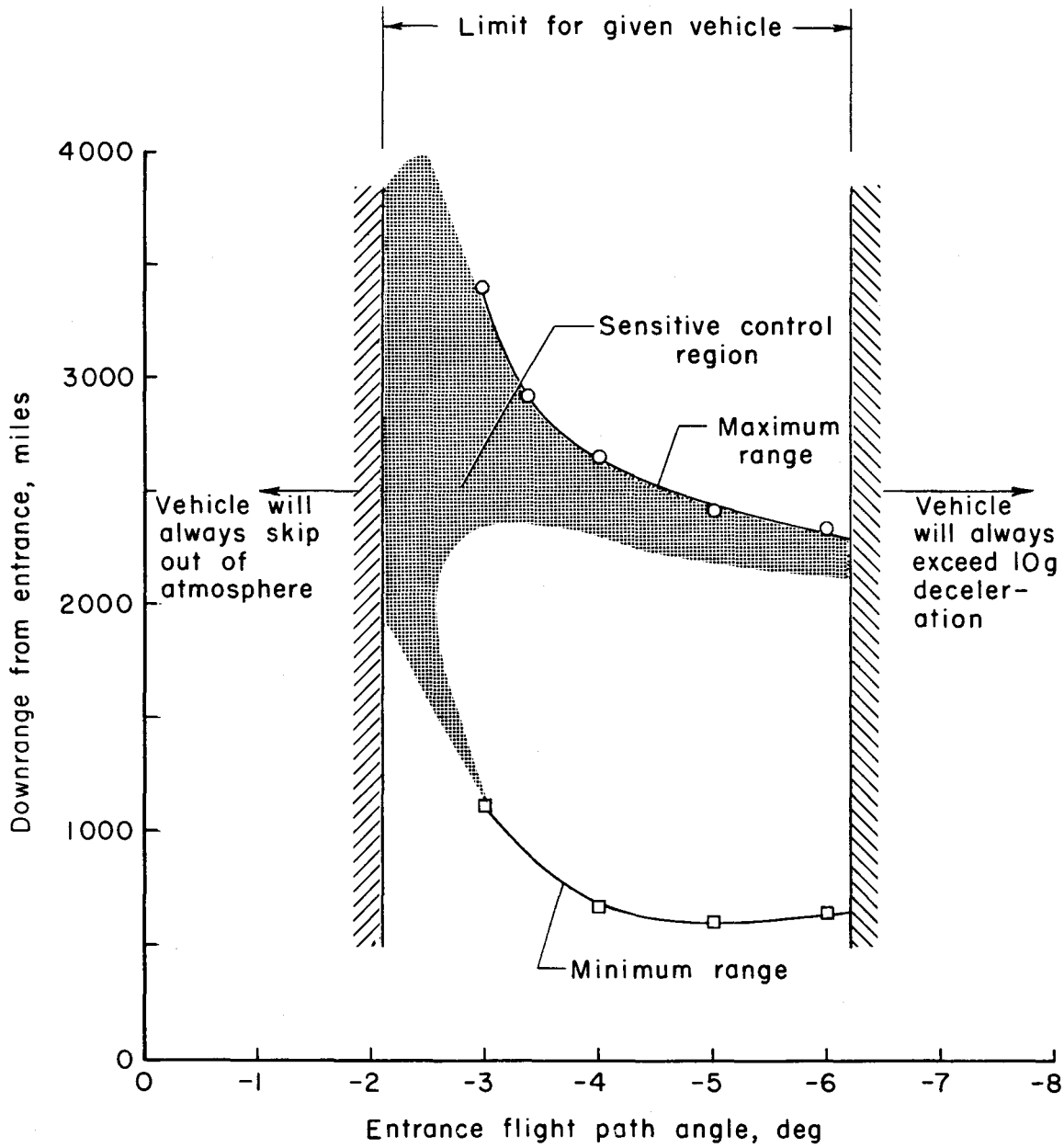

Figure 10.- Downrange and corridor boundaries for the entrance condition of $h = 290,000$ feet and $V = 35,000$ feet per second.

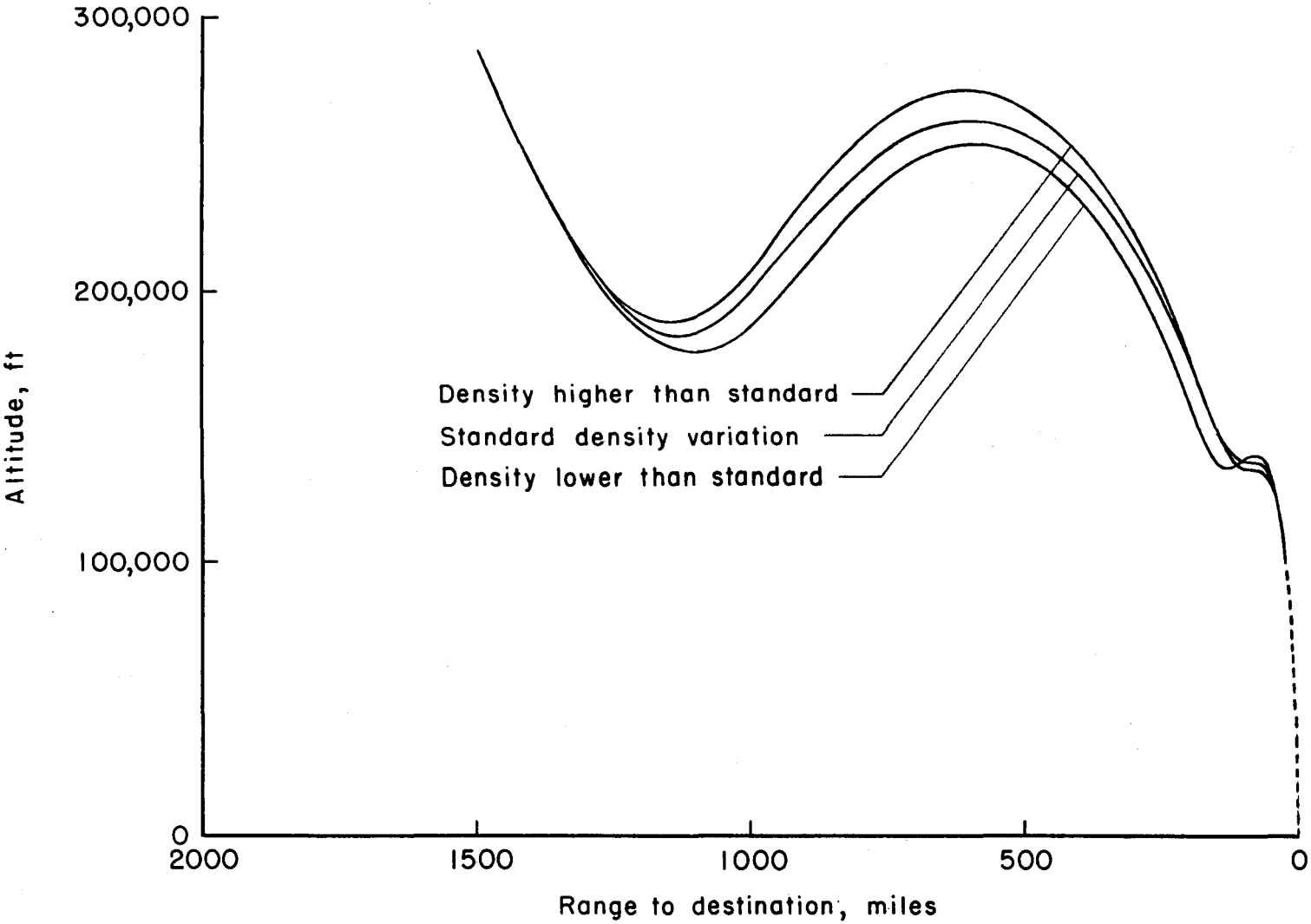

Figure 11.- Effect of density on controlled trajectory. Entry conditions: h = 290,000 feet, V = 35,000 feet per second, $\gamma = -5^{\circ}$.

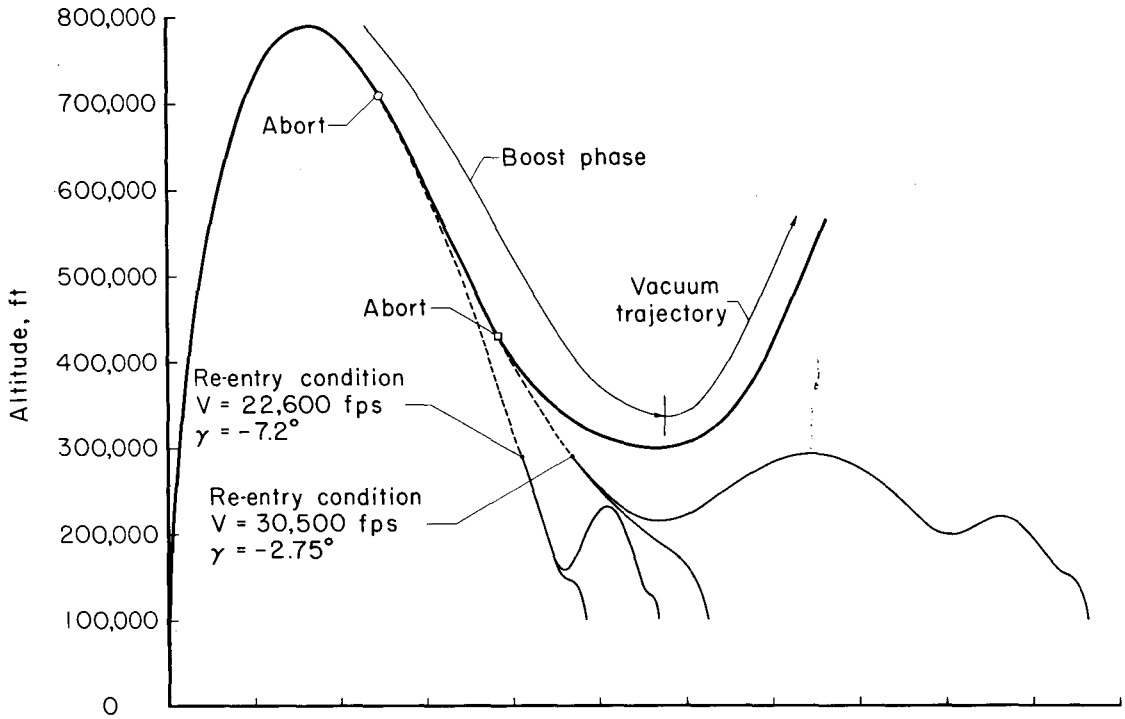

(a) Variation of range with altitude.

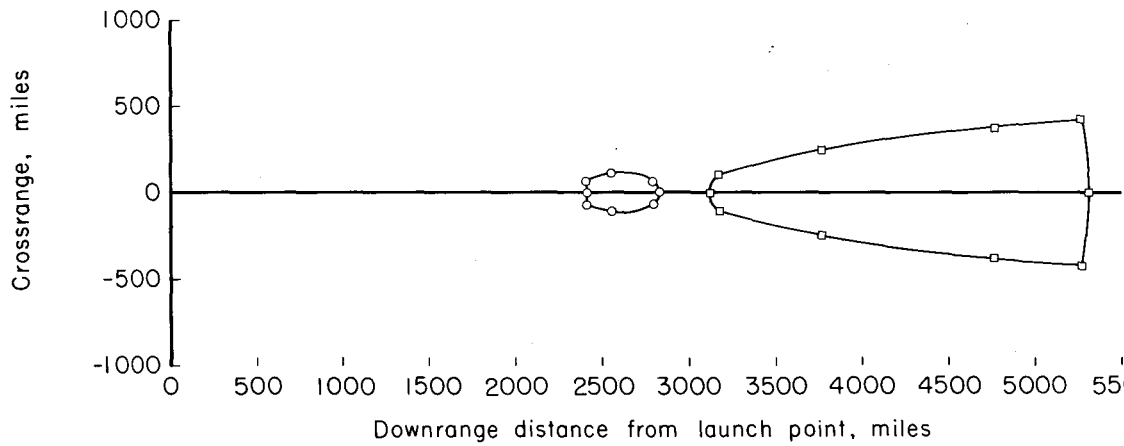

(b) Ground area attainable.

Figure 12.- Piloted trajectories for aborts from a typical lunar mission boost profile.